tvst

DOI: 10.1167/tvst.1.2.4

Article

Cellular Resolution Panretinal Imaging of Optogenetic Probes Using a Simple Funduscope

Adi Schejter[1], Limor Tsur[1], Nairouz Farah[1], Inna Reutsky-Gefen[1,2], Yishay Falick[3], and Shy Shoham[1] ✉

[1] Faculty of Biomedical Engineering, Technion - Israel Institute of Technology, Haifa, Israel
[2] Department of Medical Engineering, Ruppin Academic Center, Emek Hefer, Israel
[3] Department of Ophthalmology, Hadassah University Hospital, Ein Karem, Jerusalem, Israel

Correspondence: Shy Shoham, PhD, Faculty of Biomedical Engineering, Technion - Israel Institute of Technology, Technion City, Haifa 32000, Israel. e-mail: sshoham@bm.technion.ac.il

Received: 30 March 2012
Accepted: 10 August 2012
Published: 18 September 2012

Keywords: retinal prosthesis; gene therapy; fundus camera; fluorescent proteins; calcium indicators; Channelrhodopsin

Citation: Schejter A, Tsur L, Farah N, Reutsky-Gefen I, Falick Y, Shoham S. Cellular resolution panretinal imaging of optogenetic probes using a simple funduscope. Trans Vis Sci Tech. 2012;1(2):4, http://tvstjournal.org/doi/full/10.1167/tvst.1.2.4, doi: 10.1167/tvst.1.2.4

Purpose: To acquire and characterize cellular-resolved in vivo fluorescence images of optogenetic probes expressed in rodent retinal ganglion cells, by adapting a low-cost and simple fundus system based on a topical endoscope.

Methods: A custom endoscope-based fundus system was constructed (adapted from the design of Paques and colleagues). Bright field and fluorescence images were acquired from head-fixed transgenic mice expressing Channelrhodopsin2-eYFP, and Sprague Dawley rats virally transfected with the optogenetic probe GCaMP3. Images were compared to in vitro images of the same structures and were analyzed.

Results: The fundus system provides high-quality, high-resolution fluorescence images of the eye fundus that span the whole retina. The images allow resolving individual cells and axon bundles in the Channelrhodopsin2-eYFP mice and cellular-scale structures in the GCaMP3 expressing rats. The resolution in mouse eyes was estimated to be better than 20 μm (full width at half maximum) and is only marginally dependent on movement-related blurring.

Conclusions: The fluorescence-endoscopy fundus system provides a powerful yet simple and widely accessible tool for obtaining cellular resolved fluorescent images of optogenetic and other fluorescent probes.

Translational Relevance: The new system could prove to be a basic tool for non-invasive in vivo small animal retinal imaging in a wide array of translational vision applications, including the tracking of fluorescently tagged cells and the expression of gene-therapy and optogenetic vectors.

Introduction

Among the many emerging applications of optogenetics in neural science and technology[1] are several that are likely to have a substantial impact on translational vision technology. For example, the ability to artificially stimulate light-insensitive neurons in the retina has inspired several new concepts for vision restoration in outer retinal dystrophies.[2–6] In addition, the emergence of genetically encoded activity reporters is creating the ability to monitor responses in targeted retinal cell populations during visual information processing.[7,8] However, the widespread development of these emerging applications requires suitable tools for monitoring the expression and function of optogenetic probes, primarily in rodent models. To date, most retinal optogenetic studies of cellular-level expression and function have been conducted in vitro; however, the ability to monitor these aspects in vivo is highly desirable.

Microscopic fundus imaging in rodents is currently performed using relatively complex and expensive systems. These include scanning laser ophthalmoscopes incorporating adaptive optics[9–11] and a commercial fundus system for small animal imaging.[12,13] Two-photon microscopy also is used to look at a genetically encoded indicator in zebra fish in vivo.[8] Although these systems are, in principle, capable of microscopic fundus fluorescence imaging, their application to optogenetic cellular imaging has yet to be demonstrated, possibly because they are not easily

affordable to translational vision researchers. The current study demonstrates microscopic, cellular resolved fluorescence images of retinal ganglion cells (RGCs) expressing the optogenetic probes Channelrhodopsin2-eYFP (ChR2-eYFP) and GCaMP3 by adapting a simple and inexpensive funduscope introduced by Paques, Guyomard, Simonutti, et al.[14,15] The system's performance was characterized using physical measurements and by comparing them to in vitro acquired images of the same identified cell population.

Methods

Animal experiments were conducted in accordance with the Institutional Animal Care Committee at the Technion – Israel Institute of Technology, were in accord with the National Institutes of Health Guide for the Care and Use of Laboratory Animals, and adhered to the ARVO Statement for the Use of Animals in Ophthalmic and Vision Research.

Two strains of animals were used for different optogenetic purposes. Adult mice from a transgenic line were used: mice expressing ChR2-eYFP under a Thy1.2 promoter (7 weeks to 4 months old, strain: B6.Cg-Tg(Thy1-COP4/EYFP)9Gfng/J, Jackson Laboratories, Bar Harbor, ME). In addition, an adeno-associated virus expressing the genetically encoded calcium indicator GCaMP3 (AAV2/9.*hSynap*.G-CaMP3.3.SV40, Penn Vector Core, Philadelphia, PA) was intravitreally injected into Sprague Dawley (SD) rats (Harlan Laboratories, Rehovot, Israel). SD rats (3 to 4 weeks old) were anesthetized using a mixture of ketamine (132 mg/kgBW), xylazine (8 mg/kgBW), and acepromazine (2.8 mg/kgBW). A drop of the local anesthetic (Localine) was applied to the right eye, after which the pupil was dilated using atropine sulfate 1% (Atrospan). Then, a puncture along the cornea-sclera border was made using a 25-gauge beveled needle. Using a 31-gauge blunt needle (800 RN, Hamilton, Reno, NV), 2 μL of the virus were intravitreally injected through the previously made puncture.

Imaging was performed using an adaptation of a funduscopy system introduced by Paques, Guyomard, Simonutti, et al.[14] An endoscope with a 3 mm outer diameter otoscope and a crescent-shaped illumination (Tele Otoscope BERCI 1218 AA, Karl Storz Endoscopy, Tuttlingen, Germany) was positioned in front of a cube-mounted beam splitter (BS) or dichroic mirror (DM) (Fig. 1). A digital camera (D5000 with a Nikkor 80-200 mm f/2.8 AF-D lens, Nikon, Tokyo, Japan) was positioned perpendicular to the BS/DM. The light source was a mercury lamp (Intensilight, Nikon, Japan). The optic fiber of the light source was connected to the endoscope through a custom made adaptor, which enabled a simple introduction and replacement of optical filters. Bright field images were obtained using a 400 nm long-pass excitation filter (FGL400, Thorlabs, Newton, NJ). Fluorescence images were obtained using a 470 nm excitation filter (XF1013, Omega, Brattleboro, VT) placed in the adaptor, and a 535 nm emission filter (HQ535/50x, Chroma, Bellow Falls, VT) positioned in front of the camera lens. The camera settings typically used were image quality: raw; manual operating mode and focus (set to ∞); aperture: F2.8; ISO 3200; focal length: 110 mm. Illumination power, measured at the tip of the endoscope was between 1.5 mW and 5.5 mW, and the shutter speed was chosen according to illumination power used: for bright field images the shutter speed was set between 1/50 and 1/10 seconds, and for fluorescence images the shutter speed was set between 2 and 10 seconds.

For imaging sessions, mice were anesthetized by intraperiotoneal injection of ketamine (50 mg/kgBW) and medetomidine (1 mg/kgBW). Rats were anesthetized by intraperitoneal injection of ketamine (50 mg/kgBW), xylazine (6.25 mg/kgBW), and acepromazine (1.25 mg/kgBW). The pupils were dilated with Atrospan drops. The animals were positioned such that the eye barely touched the endoscope tip, and a drop of saline (NaCl 0.9%) was used to keep the eye hydrated and coupled with the endoscope. To minimize mouse head motion during imaging, a metal bar was surgically implanted on the skull (secured with dental acrylic), which was fastened during imaging using a miniature clamp (rats' heads were stabilized using a mouth restrainer). Raw images were processed using image processing tools (ImageJ and Photoshop, Adobe Corporation, San Jose, CA). Raw images were converted to Tiff files and the green channel was extracted. Image processing included software binning and contrast and brightness adjustments. When qualitatively comparing images acquired with different magnifications but otherwise the same parameters, the histograms of the different images were shifted to produce equal mean brightness values in order to compensate for variation in brightness levels.

Fluorescent images of isolated retinas were acquired using an inverted microscope (TE-2000U, Nikon, Japan) equipped with a charged-couple device (CCD) camera (C8484-05G, Hamamatsu Photonics,

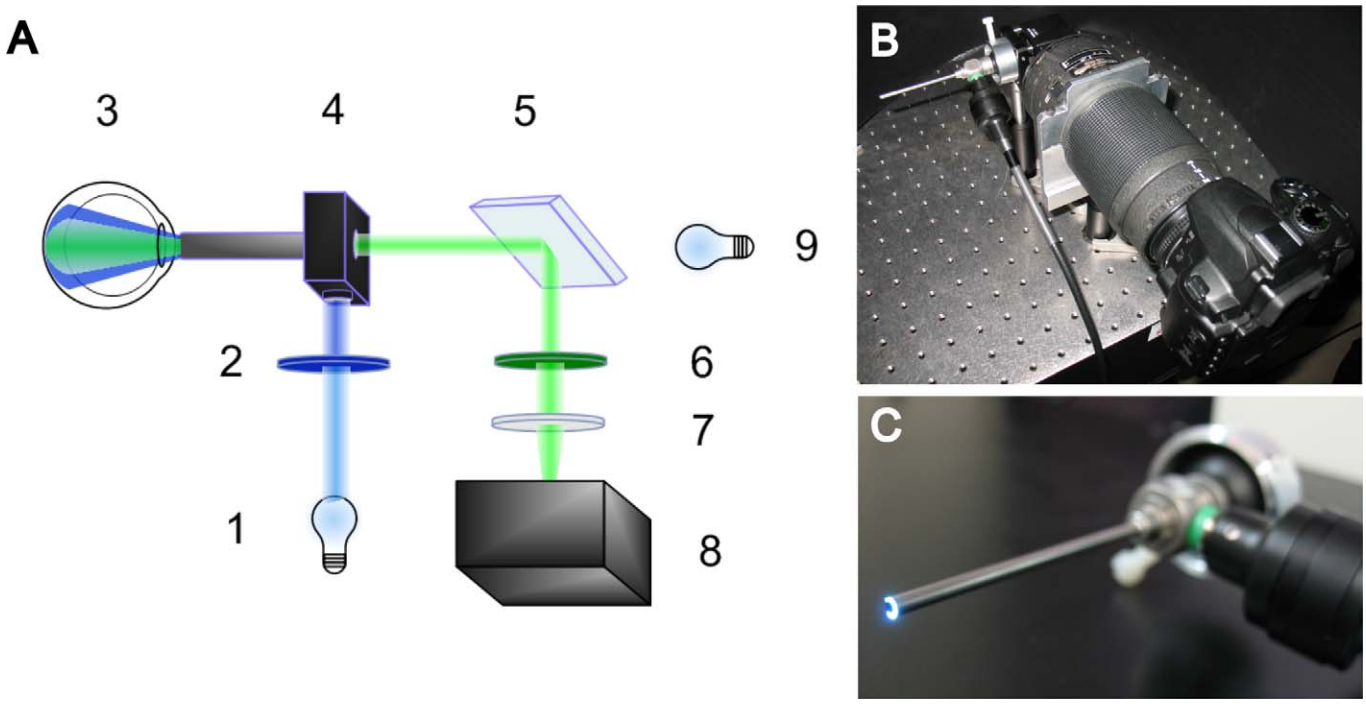

Figure 1. (A) System schematic. 1: fluorescent light source, 2: excitation filter, 3: in vivo eye, 4: endoscope, 5: DM/BS, 6: emission filter, 7: lens, 8: CCD, 9: auxiliary light source. (B) Photograph of the setup. (C) Magnification of the endoscope and custom made adaptor.

Ammersee, Germany) through a 10X (numerical aperture [NA] = 0.25) or a 20X (NA = 0.5) objective. Two-photon images were acquired using a custom-built microscope, with a 40X objective (NA = 0.8, Nikon, Japan), at a wavelength of 910 nm and a resolution of 512 × 512 pixels.

Results

To explore the system's performance characteristics, bright field and fluorescence fundus images were acquired from transgenic ChR2-eYFP-expressing mice. Representative images are in Figures 2A and B. In the fluorescence images, axons and individual RGCs could be visualized clearly (Fig. 2C), although they appeared moderately optically blurred when compared to in vitro images of isolated retinas (Fig. 2D). In these retinas the proportion of retinal ganglion cells expressing ChR2-eYFP was on the order of 30 to 40%.[16]

To test the technique's reproducibility, follow-up imaging sessions were performed after one week in the transgenic ChR2-eYFP-expressing mice. As shown in Figure 3, individual RGCs were easily identified in both imaging sessions; the slight differences between the images were due to changes in alignment of the endoscope with the dilated pupil, which led to differences in the uniformity of illumination.

The system's performance was quantitatively characterized by deriving the system's point spread function (PSF). Based on in vitro micrographs, axonal projections were assumed to have negligible diameters relative to the PSF, and therefore their observed width was used as a conservative estimate of the PSF. Intensity profiles were taken along 20 cross-sections of axonal projections from a fundus image of an anesthetized ChR2-expressing mouse, as illustrated in Figure 4A, and were fitted with a Gaussian curve, according to a minimum mean squared error criterion. The full width at half maximum (FWHM) of each of the fitted curves was evaluated (Fig. 4B) and the PSF, which was estimated as the mean FWHM, had a diameter of 18.3 ± 0.7 μm (average value ± SEM, n = 4 eyes). In order to estimate the effect of motion due to breathing on resolution (in the head-fixed animal), the PSF from a live animal (18.5 ± 1.2 μm, average value ± SEM) was compared to that of the same animal after euthanization (17.0 ± 1.5 μm, average value ± SEM). The results suggested that effects of breathing on resolution were relatively small. In order to further validate the derived PSF dimensions, an in

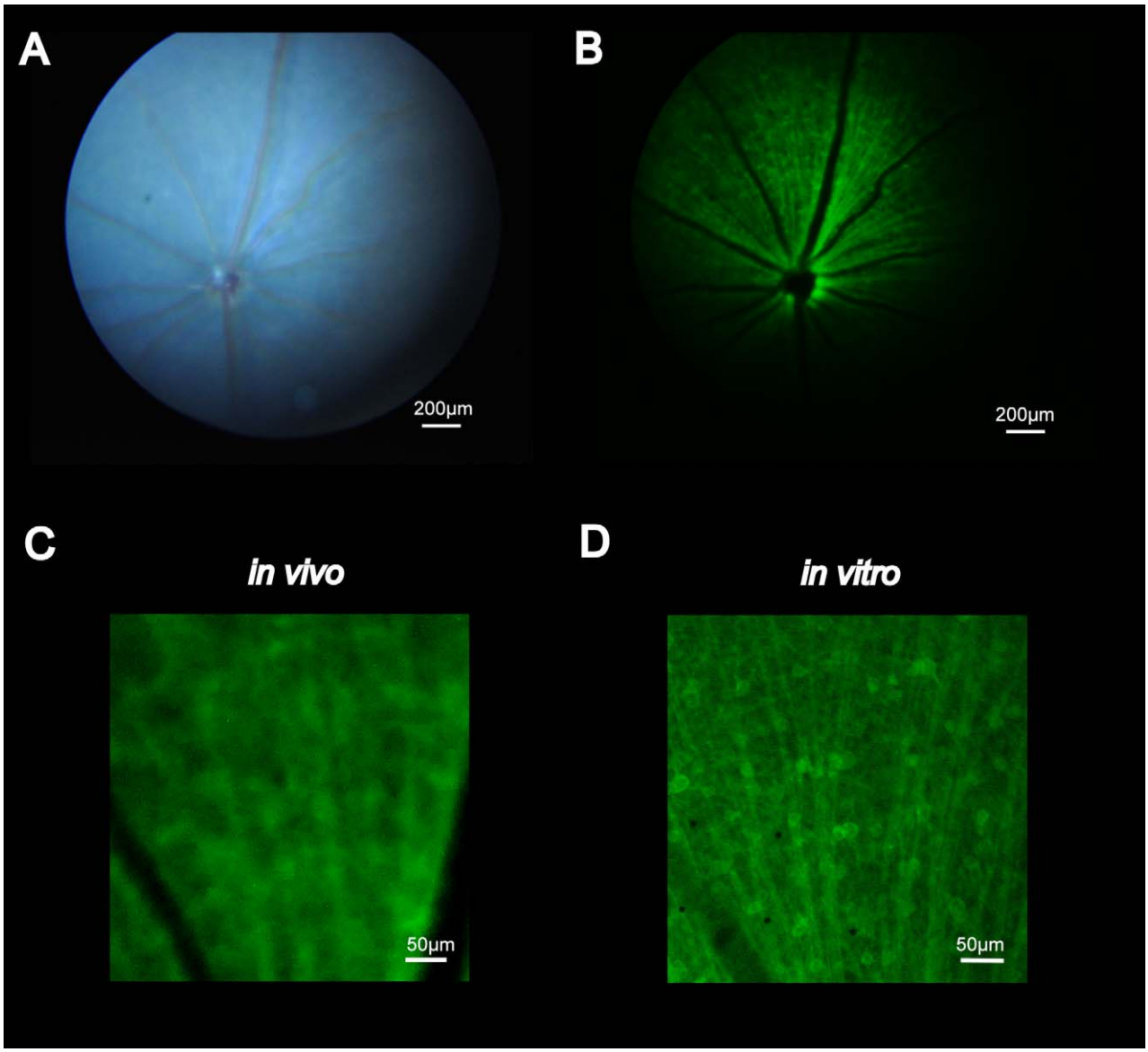

Figure 2. In vivo and in vitro images of ChR2 expressing RGCs in a B6.Cg-Tg(Thy1-COP4/eYFP) mouse. (A) Bright field fundus image and (B) fluorescent fundus image acquired in vivo. (C) Magnification of (B). (D) Fluorescent image of an isolated ChR2-expressing retina placed on a micro-electrode array.

vivo image (Fig. 4C) was compared to an image taken in vitro and blurred with a Gaussian filter with a diameter of 20.0 μm (Fig. 4D), which showed a good agreement. The effect of the camera lens' optical magnification on resolution was investigated by acquiring the same fundus scene with focal lengths of 95, 110, 135 and 200 mm (see Fig. 4E for comparison of the same cropped region). The derived PSF diameters were similar to within 5% (less than the measurement variations) and showed no trend, indicating that the optical zoom's effect on the effective resolution was minor.

Finally, the system's ability to image in vivo probes reporting cell activity was explored. Towards this end, fluorescence fundus images of GCaMP3-expressing rat retinas were also acquired (Figs. 5A through C). These examples indicated that the intravitreal viral injections resulted in a highly heterogeneous expression profile of GCaMP3 across multiple retinal layers (Figs. 5D and E show the RGC layer), with axons radiating to the optic disc (consistent with the results of Borghuis, Tian, Lu, et al).[7] Comparison of the in vivo fundus images to images acquired in vitro (Figs. 5A and B, and 5D and E, respectively) indicated that

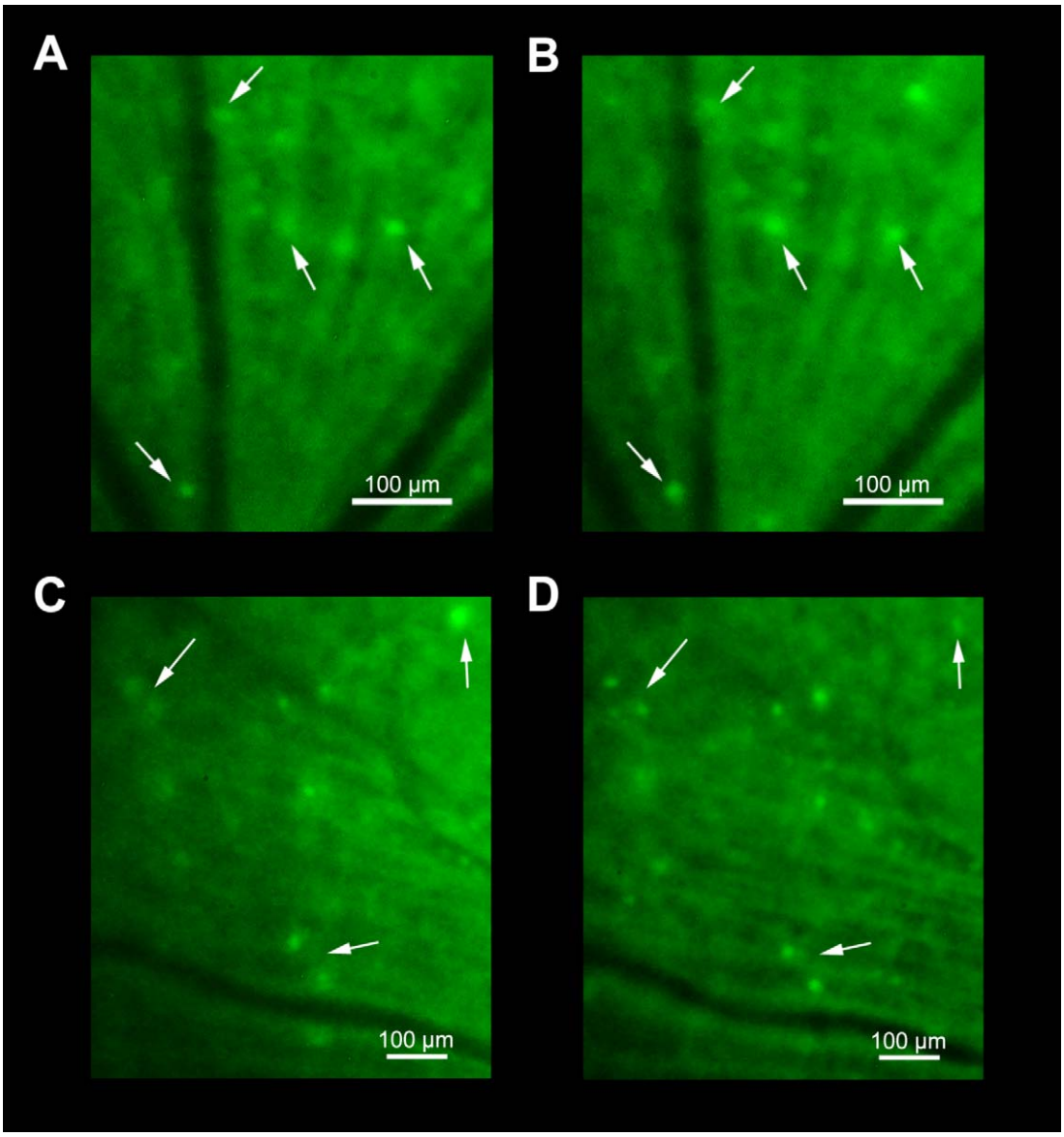

Figure 3. Repeated imaging of ChR2-eYFP expressing RGCs, separated by 1 week. (A-B), (C-D) Same subfields in two retinas; arrows indicate representative cells that were visible in both imaging sessions.

the effective resolution of the in vivo fundus images in these rats was somewhat lower, apparently only allowing the visualization of structures containing small cellular clusters.

Discussion

The in vivo acquisition of cellular-resolved fluorescence fundus images of optogenetically transduced retinal ganglion cells expressing the probes Channelrhodopsin2 and GCaMP3 have been demonstrated. The system was an adaptation of the low-cost funduscope introduced by Paques, Guyomard, Simonutti, et al,[14] but nevertheless clearly provided images with favorable resolution to those obtained using commercially available systems (compared, for example, to Dalkara, Byrne, Lee, et al,[12] in Fig. 1).

The system's performance was characterized by comparing the acquired images to in vitro images of the same population of cells. The estimated resolution in mouse eyes (Fig. 4) was better than 20 µm (FWHM), and clearly allowed distinguishing single identified cells. This resolution could be further improved by applying offline image processing

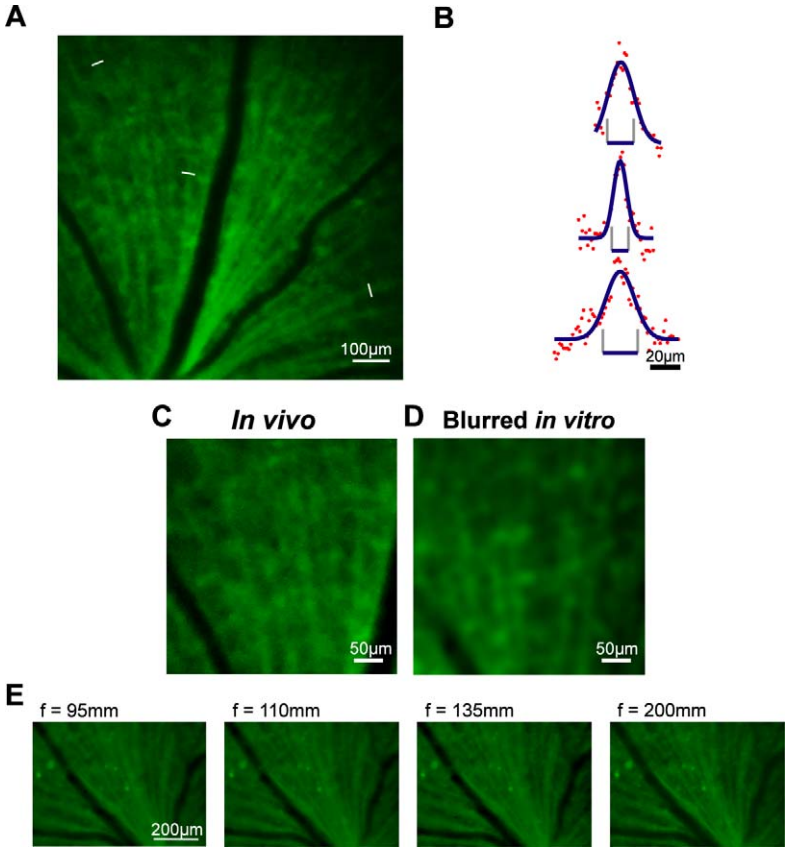

Figure 4. Evaluation of the system's resolution performance. (A) Fluorescent fundus image of ChR2-eYFP expressing RGCs in a B6.Cg-Tg(Thy1-COP4/eYFP) mouse. White markings illustrate lines along which intensity profiles of axons may be taken. (B) Three intensity profiles taken along the cross-sections of different axons fitted with Gaussian curves. Bars below illustrate the FWHM of the curves. (C) Enlarged fundus image (same retina as in (A)). (D) In vitro fluorescent image of an isolated ChR2-eYFP expressing retina (same as in Fig. 2D), blurred with a Gaussian filter, FWHM = 20.0 μm. (E) Magnified area cropped from fundus images captured at focal lengths: 95, 110, 135, and 200 mm (left to right). The effective resolution appears similar, consistent with quantitative measurements.

techniques including deconvolution. An additional set of experiments investigated the source of this effective resolution. It was found that the resolution in head-fixed mice was only modestly improved (by approximately 10%) when motion was completely eliminated, but strongly deteriorated when the head was not fixated (not shown). This suggested that the effective resolution was primarily limited by the optical point spread function, and appeared to be relatively independent of the optical zoom in the effective range of the lens. Because image truncation occurs for f greater than 110 mm, this value was often chosen in practice.

The ability to image cellular-resolved optogenetic probes in rodent retinas using a simple and highly accessible technique could facilitate the development of translational strategies for vision restoration. The system's high resolution imaging capability could also prove advantageous for noninvasive in vivo tracking of fluorescently tagged cells, monitoring the expression of gene-therapy vectors, and observing the development of retinal dystrophies and retinal plaques that develop in Alzheimer's disease.[13] Moreover, the system design could allow for light stimuli to be projected onto the retina through the endoscope. When combined with genetically encoded activity reporters, this could enable a powerful strategy for imaging cellular-resolved evoked activity patterns.

Acknowledgments

The authors thank the European Research Council (grant #211055) for financial support; Bart Borghuis, Inbar Brosh, Thierry Wasserman, Amit Oved, and Shem-Tov Halevi for their advice and assistance; and Loren L. Looger and the Janelia Farm Research

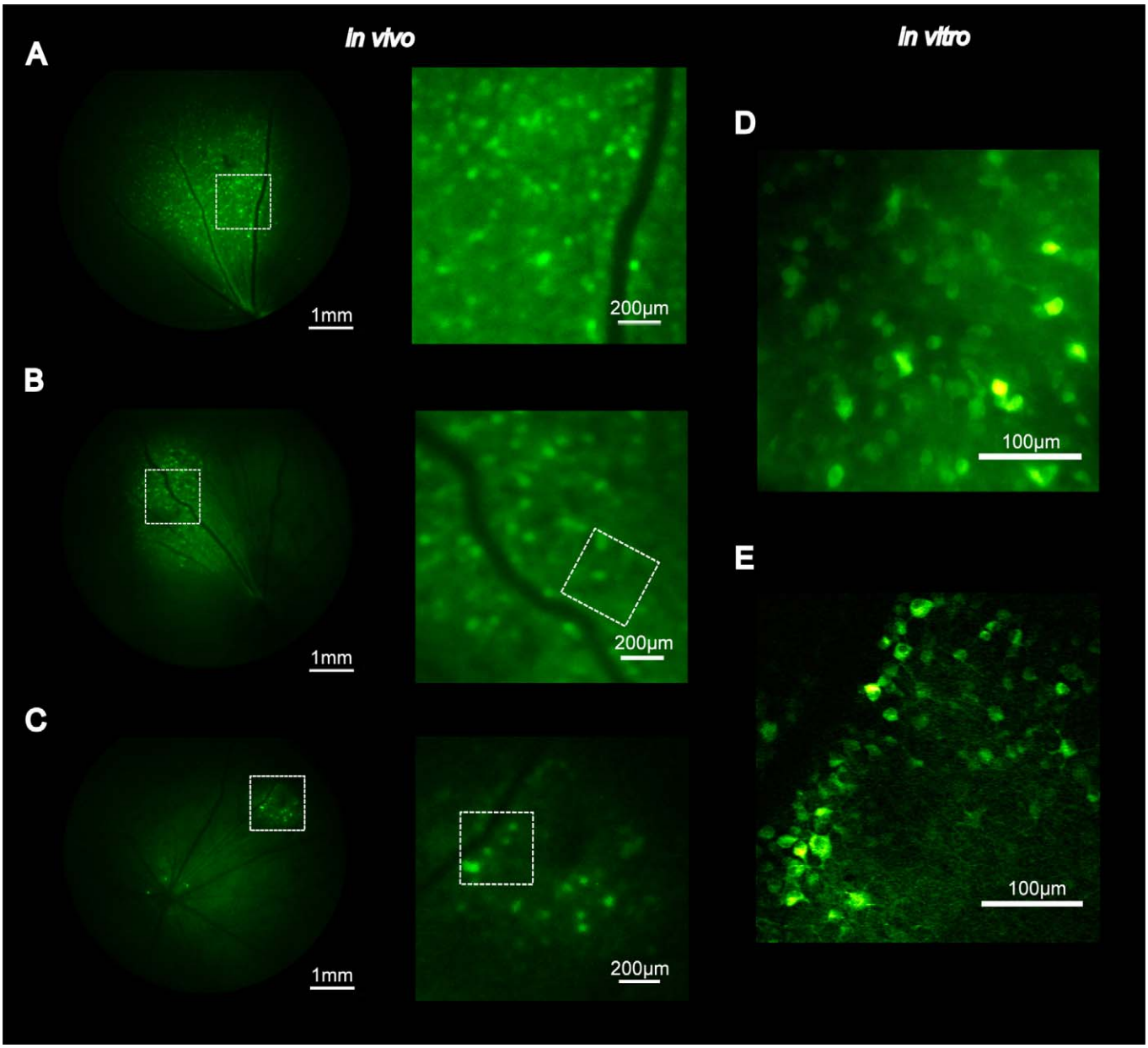

Figure 5. In vivo and in vitro fluorescence fundus images of GCaMP3-expressing RGCs in SD rats. (A)-(C) Left: fluorescence fundus images, right: magnification of the area indicated in left panel. (D) In vitro epifluorescence microscope image of the whole-mount retina isolated from the eye in (B). (E) Two-photon laser-scanning image of retina isolated from (C). The respective magnified fields are marked.

Campus of the Howard Hughes Medical Institute for permission to use GCaMP3.

Financial support: European Research Council (grant no. 211055)

Disclosure: **A. Schejter,** None; **L. Tsur,** None; **N. Farah,** None; **I. Reutsky-Gefen,** None; **Y. Falick,** None; **S. Shoham,** None

References

1. Yizhar O, Fenno LE, Davidson TJ, Mogri M, Deisseroth K. Optogenetics in neural systems. *Neuron*. 2011;71(1):9–34.
2. Bi A, Cui J, Ma YP, Olshevskaya E, Pu M, Dizhoor AM, et al. Ectopic expression of a microbial-type rhodopsin restores visual responses in mice with photoreceptor degeneration. *Neuron*. 2006;50(1):23–33.

3. Tomita H, Sugano E, Yawo H, Ishizuka T, Isago H, Narikawa S, et al. Restoration of visual response in aged dystrophic RCS rats using AAV-mediated channelopsin-2 gene transfer. *Invest Ophthalmol Vis Sci*. 2007;48(8):3821–3826.
4. Lagali PS, Balya D, Awatramani GB, Munch TA, Kim DS, Busskamp V, et al. Light-activated channels targeted to ON bipolar cells restore visual function in retinal degeneration. *Nat Neurosci*. 2008;11(6):667–675.
5. Busskamp V, Roska B. Optogenetic approaches to restoring visual function in retinitis pigmentosa. *Curr Opin Neurobiol*. 2011;21(6):942–946.
6. Doroudchi MM, Greenberg KP, Liu J, Silka KA, Boyden ES, Lockridge JA, et al. Virally delivered channelrhodopsin-2 safely and effectively restores visual function in multiple mouse models of blindness. *Mol Ther*. 2011;19(7):1220–1229.
7. Borghuis BG, Tian L, Xu Y, Nikonov SS, Vardi N, Zemelman BV, et al. Imaging light responses of targeted neuron populations in the rodent retina. *J Neurosci*. 2011;31(8):2855–2867.
8. Dreosti E, Esposti F, Baden T, Lagnado L. In vivo evidence that retinal bipolar cells generate spikes modulated by light. *Nat Neurosci*. 2011; 14(8):951–952.
9. Roorda A, Romero-Borja F, Donnelly III W, Queener H, Hebert T, Campbell M. Adaptive optics scanning laser ophthalmoscopy. *Opt Express*. 2002;10(9):405–412.
10. Leung CK, Lindsey JD, Crowston JG, Ju WK, Liu Q, Bartsch DU, et al. In vivo imaging of murine retinal ganglion cells. *J Neurosci Methods*. 2008;168(2):475–478.
11. Gray DC, Merigan W, Wolfing JI, Gee BP, Porter J, Dubra A, et al. In vivo fluorescence imaging of primate retinal ganglion cells and retinal pigment epithelial cells. *Opt Express*. 2006; 14(16):7144–7158.
12. Dalkara D, Byrne LC, Lee T, Hoffmann NV, Schaffer DV, Flannery JG. Enhanced gene delivery to the neonatal retina through systemic administration of tyrosine-mutated AAV9. *Gene Ther*. 2011;19(2):176–181.
13. Koronyo-Hamaoui M, Koronyo Y, Ljubimov AV, Miller CA, Ko MK, Black KL, et al. Identification of amyloid plaques in retinas from Alzheimer's patients and noninvasive in vivo optical imaging of retinal plaques in a mouse model. *Neuroimage*. 2011;54(suppl 1):S204–217.
14. Paques M, Guyomard JL, Simonutti M, Roux MJ, Picaud S, Legargasson JF, et al. Panretinal, high-resolution color photography of the mouse fundus. *Invest Ophthalmol Vis Sci*. 2007;48(6): 2769–2774.
15. Guyomard JL, Rosolen SG, Paques M, Delyfer MN, Simonutti M, Tessier Y, et al. A low-cost and simple imaging technique of the anterior and posterior segments: eye fundus, ciliary bodies, iridocorneal angle. *Invest Ophthalmol Vis Sci*. 2008;49(11):5168–5174.
16. Thyagarajan S, van Wyk M, Lehmann K, Lowel S, Feng G, Wassle H. Visual function in mice with photoreceptor degeneration and transgenic expression of channelrhodopsin 2 in ganglion cells. *J Neurosci*. 2010;30(26):8745–8758.